View Article Online / Journal Homepage / Table of Contents for this issue
Dynamic Article Links

Journal of Materials Chemistry

Cite this: *J. Mater. Chem.*, 2011, **21**, 5475

www.rsc.org/materials

PAPER

Hypercrosslinked organic polymer networks as potential adsorbents for pre-combustion CO_2 capture

Claudia F. Martín,[a] Ev Stöckel,[b] Rob Clowes,[c] Dave J. Adams,[b] Andrew I. Cooper,[bc] Jose J. Pis,[a] Fernando Rubiera[a] and Cova Pevida*[a]

Received 19th October 2010, Accepted 7th February 2011
DOI: 10.1039/c0jm03534c

Published on 25 February 2011. Downloaded by Pennsylvania State University on 18/05/2016 03:58:11.

Hypercrosslinked polymers (HCPs) synthesized by copolymerisation of *p*-dichloroxylene (*p*-DCX) and 4,4′-bis(chloromethyl)-1,1′-biphenyl (BCMBP) constitute a family of low density porous materials with excellent textural development. Such polymers show microporosity and mesoporosity and exhibit Brunauer–Emmett–Teller (BET) surface areas of up to 1970 $m^2\ g^{-1}$. The CO_2 adsorption capacity of these polymers was evaluated using a thermogravimetric analyser (atmospheric pressure tests) and a high-pressure magnetic suspension balance (high pressure tests). CO_2 capture capacities were related to the textural properties of the HCPs. The performance of these materials to adsorb CO_2 at atmospheric pressure was characterized by maximum CO_2 uptakes of 1.7 mmol g^{-1} (7.4 wt%) at 298 K. At higher pressures (30 bar), the polymers show CO_2 uptakes of up to 13.4 mmol g^{-1} (59 wt%), superior to zeolite-based materials (zeolite 13X, zeolite NaX) and commercial activated carbons (BPL, Norit R). In addition, these polymers showed low isosteric heats of CO_2 adsorption and good selectivity towards CO_2. Hypercrosslinked polymers have potential to be applied as CO_2 adsorbents in pre-combustion capture processes where high CO_2 partial pressures are involved.

1. Introduction

Carbon Capture and Storage (CCS) technologies offer potential for diminishing CO_2 emissions in the atmosphere. Adsorption is considered a promising technology for CO_2 capture, offering possible energy savings compared to other more established absorption technologies.[1,2] Different types of solid sorbents have been investigated as potential adsorbents for CO_2 capture. These include supported amines,[3–6] carbon-based sorbents,[7–14] supported carbonates[15,16] and zeolites.[17–19] Based on the nature of the bonding between the adsorbate molecule and the solid surface, adsorption can be categorized as either physical or chemical. Most adsorptive separation processes depend on physical adsorption rather than chemical adsorption. The requirement for adequate adsorptive capacity restricts the choice of adsorbent for practical separation processes to microporous adsorbents with pore diameters ranging from 2–3 nm. Previous studies have shown that only pores smaller than five times the molecular size of the adsorbate are effective for gas adsorption at atmospheric pressure. This observation was confirmed empirically[20] as well as by mathematical simulation using grand canonical Monte Carlo (GCMC) and the non-local density functional theory (NLDFT).[21] Since the molecular size of CO_2 is 0.209 nm, only pores less than 1.0 nm are effective towards CO_2 capture at atmospheric pressure.[22] However, at higher pressures, CO_2 is also adsorbed in the supermicroporosity range (pore sizes between 0.7 and 2 nm).[22]

The work presented here is based on the synthesis of solid adsorbents with the potential to be applied in pre-combustion CO_2 capture—that is, the removal of CO_2 from shifted-syngas prior to electricity generation with additional production of high-purity H_2. Solid sorbents are currently used in pressure swing adsorption (PSA) systems for the purification of hydrogen in petrochemical industries.[2,23,24] The synthesis gas or hydrogen is used as fuel or chemical raw material: for example, in liquid-fuel manufacturing or ammonia synthesis. The CO_2 can also be used as a chemical raw material for dry ice manufacturing, carbonated beverage production,[25,26] treatment of alkaline water, dry cleaning processes (supercritical CO_2)[27] or in enhanced oil recovery (EOR) from oil wells.[28]

Regarding PSA processes using solid sorbents, recent studies reveal the increased interest of this technology for pre-combustion CO_2 capture applications, due to the reduced size of the capture system and the increased CO_2 partial pressure when compared to post-combustion capture.[29,30]

There is currently significant interest in the use of porous networks for gas storage and trapping applications.[31–35] There are a few different classes of microporous organic polymers (MOPs)[36] including hypercrosslinked polymers (HCPs),[37–41] polymers of intrinsic microporosity (PIMs),[42,43] conjugated

[a]*Instituto Nacional del Carbón (INCAR), CSIC, Apartado 73, 33080 Oviedo, Spain. E-mail: cpevida@incar.csic.es*
[b]*University of Liverpool, Robert Robinson Laboratories, Crown Street, Liverpool, L69 7ZD, UK*
[c]*Centre for Materials Discovery, Crown Street, Liverpool, L69 7ZD, UK*

View Article Online

Published on 25 February 2011. Downloaded by Pennsylvania State University on 18/05/2016 03:58:11.

microporous polymers (CMPs),[44–47] and covalent organic frameworks (COFs).[32] MOPs can be classified as either amorphous (HCPs, PIMs, CMPs) or crystalline (COFs).[36] A possible advantage of MOPs, compared to other microporous materials such as MOFs, zeolites and activated carbons, is the potential synthetic diversity that can be incorporated into these organic structures.[46]

HCPs represent a family of robust microporous organic materials that can exhibit high surface areas.[37–39,41,48,49] Unlike solution-processable PIMs, the permanent porosity in hypercrosslinked materials is a result of extensive crosslinking reactions which prevent the polymer chains from collapsing into a dense, non-porous state.[50,51] The most well-studied hypercrosslinked materials are "Davankov-type" resins,[39,48,49] prepared by post-crosslinking of polystyrenic networks. These materials can exhibit apparent BET surface areas as high as 2090 $m^2\ g^{-1}$ (ref. 52) and have been used as sorbents for organic vapours,[53] for the recovery of organic compounds from water,[54] and in chromatography.[55] Among other features, the HCPs present robustness and scalability; these materials have good thermal stability, excellent chemical robustness (*e.g.*, to strong acids and bases), and are quite readily produced on a large scale. In addition, they can be produced in a molded monolithic form. Another distinct advantage of the HCPs is their relative low heat of adsorption in comparison with other materials. We have recently reported the synthesis of HCPs by the self-condensation of bischloromethyl monomers such as dichloroxylene (DCX) and 4,4′-bis(chloromethyl)-1,1′-biphenyl (BCMBP).[40] These HCPs were predominantly microporous and exhibited Brunauer–Emmett–Teller (BET) surface areas of up to 1904 $m^2\ g^{-1}$. Networks based on BCMBP exhibited a gravimetric H_2 storage capacity of 3.68 wt% at 15 bar and 77.3 K.[40] We were also able to carry out atomistic simulations of gas sorption in these networks.[56] In this work, HCP networks have been evaluated for CO_2 capture under either atmospheric (post-combustion capture conditions) or high pressure (pre-combustion capture conditions). The results indicate that HCPs can be considered as promising materials for the separation of CO_2 under pre-combustion capture conditions.

2. Experimental

2.1. Chemicals

α,α′-Dichloro-*p*-xylol (*p*-DCX, Aldrich, 98%), 4,4′-bis(chloromethyl)-1,1′-biphenyl (BCMBP, Aldrich, 95%), and iron(III) chloride anhydrous ($FeCl_3$, Alfa Aesar-Johnson Matthey Company, 98%,) were used as received. As solvents, dodecane (99%), cyclohexane (99%) and *n*-hexane (99%) were purchased from Fischer Scientific. Dichloroethane (DCE, 99.8%, anhydr.) was purchased from Sigma Aldrich. All solvents were used as received.

2.2. General synthesis of HCPs (see Table 1 for % mol mol^{-1} ratios for individual reactions)

To a solution of monomer(s) in anhydrous dichloroethane (DCE, 5 mL), a slurry of $FeCl_3$ (0.7 g, 4.3 mmol) in DCE (5 mL) was added under nitrogen atmosphere. The resulting mixture was heated while stirring at 353 K for 18 h. The resulting brown precipitate was washed well with water and methanol until the filtrate became clear and then finally with diethyl ether. The polymer was dried under vacuum for 24 h at 333 K.

***Safety Note**: Friedel–Crafts chemistry can be strongly exothermic and can lead to rapid temperature ramps. These reactions can generate very substantial pressures if carried out in sealed tubes.*

2.3. Characterization of the polymers

The synthesized polymers were characterized in terms of texture and chemical composition. For the textural characterization, the specific surface areas and micropore volumes were determined from the N_2 and CO_2 adsorption isotherms at 77 K and 273 K, respectively, measured in a Micromeritics ASAP 2420. Nitrogen surface areas were calculated by means of the BET equation and micropore volumes were determined from the Dubinin–Radushkevich (DR) equation applied to the CO_2 and N_2 adsorption isotherms.[59] Helium densities at 308 K were measured in a Micromeritics Accupyc 1330 pycnometer. Prior to any measurement, the samples were degassed under vacuum at 373 K for approximately 10 h.

Previous studies on the reproducibility of the synthesis of the HCPs (*i.e.*, repeat reactions under the same conditions), showed some variation in both yield and surface area,[40] possibly because of the propensity for these exothermic reactions to form "hot spots" and the general difficulty in controlling this on a small test scale (<2 g solids). By contrast, the reproducibility of the gas sorption measurements was found to be excellent (±3%).

The chemical characterization involved microanalysis. Heats of CO_2 adsorption were determined in the Micromeritics ASAP 2420 from the experimentally measured CO_2 adsorption isotherms at 273 and 298 K up to a pressure of 1.13 bar.

2.4. Assessment of the CO_2 capture capacity

The CO_2 adsorption capacity of the samples at atmospheric pressure was evaluated in a thermogravimetric analyser (Setaram TGA). In a typical experiment, a sample (~20 mg) was loaded in the TGA and dried at 373 K under inert atmosphere of argon (50 mL min^{-1}) prior to the adsorption experiment. The system was then cooled to room temperature and, after stabilization of the sample mass and temperature (298 K), the argon flow was changed to CO_2 (50 mL min^{-1}). The CO_2 adsorption capacity at 298 K was assessed from the maximum mass increase of the samples when exposed to a pure CO_2 atmosphere.

The CO_2 adsorption capacity at higher pressures was evaluated in a high-pressure magnetic suspension balance (Rubotherm-VTI). Firstly, the samples were degassed at 373 K for 120 min under vacuum. Then, the system was cooled down to room temperature and sequentially pressurized (pressure steps ≈ 2.5 bar) under CO_2 atmosphere from 0.2 to 30 bar allowing to reach adsorption equilibrium. In this way, the CO_2 adsorption isotherms at 298 K were determined. The CO_2 uptake at each pressure was interpreted as the maximum CO_2 adsorption capacity. In addition, H_2 adsorption isotherms at 298 K up to a pressure of 40 bar were also determined following the same procedure.

 This journal is © The Royal Society of Chemistry 2011

View Article Online

Published on 25 February 2011. Downloaded by Pennsylvania State University on 18/05/2016 03:58:11.

The selectivity of the prepared HCPs to separate CO_2 from CO_2/H_2 mixtures was estimated by the ratio between the CO_2 and H_2 adsorption capacities at a selected pressure.

3. Results and discussion

3.1. Chemical and textural characterization

Following our previous report,[40] a series of HCPs was prepared *via* the self-condensation of two bischloromethyl monomers, dichloroxylene (DCX) and 4,4′-bis(chloromethyl)-1,1′-biphenyl (BCMBP) (Table 1 and Fig. 1). Previous work was carried out using dichloroethane (DCE) as a suitable solvent. For optimisation purposes and to compare the previous synthesis with 'greener' systems, the synthesis of HCPs was also attempted in alternative solvents.

Microanalysis of the polymers is included in Table 2. The prepared HCPs contain mainly carbon (80–86 wt%), the analysis being in agreement with the work carried out previously.[40] It can be observed that all samples have similar chemical compositions. We have previously demonstrated strong solvent effects for Sonogashira–Hagihara coupling based microporous materials.[57] This was ascribed to better monomer solubilities promoting reactivity. Presumably, networks with higher degrees of condensation are less able to collapse and densify, thus leading to higher levels of microporosity. It is likely that the same effects are being observed here. Indeed, the lower percentage of carbon found in samples 5–7 as compared to samples 1–4 (Table 2) as well as the lower C/H ratio may be indicative of lower degrees of condensation and the presence of chlorine end groups. Additionally, the differences observed between samples 5–7 and 1–4 may be related to the solvation or lack of solvation by the different potentially porogenic solvents, as rationalized by Sherrington.[58]

Fig. 2 and 3 show the N_2 and CO_2 adsorption isotherms at 77 and 273 K, respectively, for the synthesized polymers. Table 3 summarizes the textural parameters calculated from these isotherms. BET surface areas (S_{BET}) were estimated in the relative pressure range between 0.00003 and 0.3. Total pore volume (V_p) was evaluated using the Gurvitch's rule ($p/p^0 = 0.99$). The mesopore volume (V_{meso}) was calculated by the Hybrid Density Functional Theory (DFT), assuming cylindrical pores in pillared clay,[60] non-regularization and medium smoothing. Micropore volumes, W_{0,N_2} (total micropore volume, estimated at relative pressures < 0.1) and W_{0,CO_2} (narrow micropore volume, estimated at relative pressures < 0.01) were calculated by the DR equation[59] applied to the N_2 and CO_2 adsorption isotherms (assuming affinity coefficients of 0.33 for N_2 and 0.36 for CO_2). Average widths of the narrow micropores, L_{0,CO_2}, were estimated applying the Stoeckli–Ballerini relation to the CO_2 adsorption isotherms.[61]

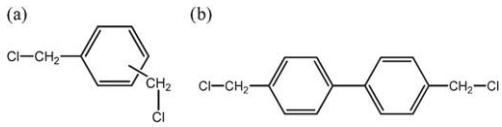

Fig. 1 Monomers used for the synthesis of the hypercrosslinked polymer networks: (a) DCX: α,α′-dichloro-*p*-xylene and (b) BCMBP: 4,4′-bis-(chloromethyl)-1,1′-biphenyl.

Polymers 1 to 4 showed type IV N_2 adsorption isotherms, according to the BDDT classification,[62] characterized by the presence of a hysteresis loop at relative pressures above 0.4. This suggests the presence of significant mesoporosity besides microporosity. Great similarities in N_2 adsorption up to relative pressures around 0.4 were observed. However, hysteresis loops at higher relative pressures show differences and so does the mesoporosity in the samples. Samples 5, 6 and 7 showed negligible N_2 adsorption. Polymer 4 showed the greatest N_2 uptake.

Fig. 3 shows the CO_2 adsorption isotherms at 273 K for HCPs (1 to 7). Sub-atmospheric CO_2 adsorption isotherms at 273 K allow the evaluation of microporosity with pore sizes of less than 1 nm. Differences in the volumes of CO_2 adsorbed and the shape of the isotherms can be observed. Polymers 5, 6 and 7 showed little adsorption of CO_2 with curved isotherms that suggest the presence of narrow micropore distributions. Samples 1 to 4 presented similar CO_2 isotherms characterized by rectilinear shape that indicates the presence of wider micropores. The highest CO_2 uptake corresponded to sample 4.

The textural parameters calculated from the N_2 and CO_2 adsorption isotherms are summarized in Table 3. The absolute densities measured at 308 K for all HCPs were recorded to be around 1 g cm^{-3}. The HCPs synthesized using cyclohexane, *n*-hexane and dodecane as solvents (polymers 5, 6 and 7) showed negligible total pore volume and BET surface areas. Polymers 1 to 4, synthesized with DCE, showed S_{BET} values around 1600 m^2 g^{-1}, slightly lower than those previously reported,[40] and micropore volumes, W_{0,N_2}, around 0.6 cm^3 g^{-1}. Mesoporosity in these polymers showed more dispersion with mesopore volumes ranging from 0.3 to 0.5 cm^3 g^{-1}. Polymer 4 exhibited the lowest mesopore volume but the greatest total pore volume.

Regarding the evaluation of narrow microporosity it can be observed in Table 3 that values around 0.3 cm^3 g^{-1} and 0.9 nm for the narrow micropore volume, W_{0,CO_2}, and average narrow micropore width, L_{0,CO_2}, respectively, were obtained. From these results, it can be concluded that replacement of DCE by alkane solvents in the HCP synthesis does not enhance the textural development. However, the ratio DCX/BCMBP during the synthesis may influence the development of mesoporosity in the polymers.

Table 1 Details on the synthesis of the series of hypercrosslinked polymers (monomer ratios given in % mol mol^{-1})

Sample	DCX	BCMBP	DCX/g	BCMBP/g	$FeCl_3$/g	DCE/mL	Cyclo-hexane/mL	*n*-Hexane/mL	Dodecane/mL
1	0	100	0.00	1.069	0.696	10	—	—	—
2	25	75	0.188	0.804	0.688	10	—	—	
3	50	50	0.380	0.537	0.699	10	—	—	—
4	75	25	0.570	0.269	0.704	10	—	—	—
5	25	75	0.185	0.806	0.687	—	10	—	—
6	25	75	0.187	0.806	0.708	—	—	10	—
7	25	75	0.189	0.806	0.690	—	—	—	10

View Article Online

Published on 25 February 2011. Downloaded by Pennsylvania State University on 18/05/2016 03:58:11.

Table 2 Chemical characteristics of HCPs

	Ultimate microanalysis (wt%, db)	
Sample	C	H
1	83.71	5.22
2	86.28	5.27
3	83.09	5.30
4	81.56	5.34
5	78.41	6.13
6	80.96	5.29
7	79.51	5.53

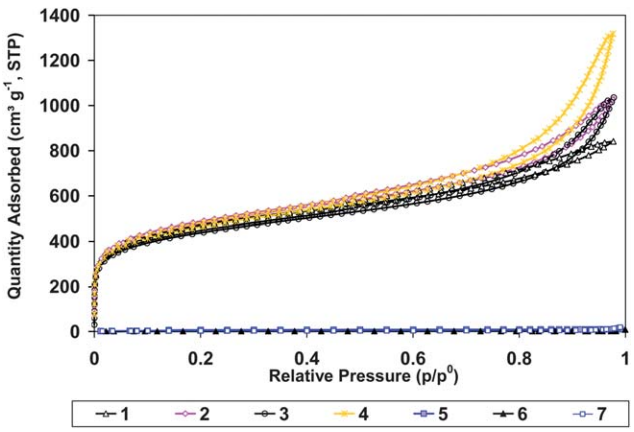

Fig. 2 N_2 adsorption isotherms at 77 K for HCPs.

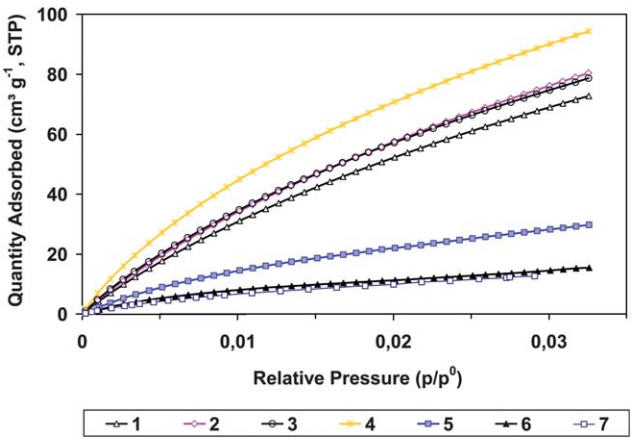

Fig. 3 CO_2 adsorption isotherms at 273 K for HCPs.

Fig. 4 shows the pore size distribution assessed by the Hybrid DFT method, assuming a model of cylindrical pores in pillared clay. In general, polymers presented here showed pore size distributions with maxima centered in the supermicroporosity range (2 nm > micropore width > 0.7 nm), in agreement with the average micropore widths (0.8–0.9 nm) determined from the Stoeckli–Ballerini relation (see Table 3).

3.2. Isosteric heat of adsorption of CO_2

The isosteric heat of adsorption (Q_{st}), which is defined as the difference in the partial molar enthalpy of the adsorbate between the gas phase and the adsorbed phase, represents the strength of the adsorbate–adsorbent interactions. Quantification of Q_{st} is very important for the design of adsorption processes because the heat released upon adsorption is partially adsorbed on the sorbent which causes a rise in the sorbent temperature and thus influences the local adsorption equilibrium and kinetics and, as a result, the overall gas separation efficiency.[63] Adsorption isotherms of CO_2 were obtained at different temperatures, 273 K and 298 K, and were used for the calculation of the isosteric heat of adsorption, based on the Clausius–Clapeyron equation.[64] The isosteric heats of adsorption are plotted in Fig. 5 as a function of the amount of CO_2 adsorbed.

In Fig. 5 it can be observed that at lower loadings (<20 $cm^3\ g^{-1}$, STP) the performance of the samples differs and the heats of adsorption can slightly increase (polymers 3 and 4), decrease (polymer 2) or stay constant (polymer 1). This behaviour may be assigned to uncertainties in the evaluation procedure because at very low pressures, the isotherm measurements at lower temperatures may not be precise for strongly adsorbed gases.[65] However, at higher loadings the heats of adsorption of CO_2 reach nearly constant values with loading of approximately 21 kJ mol^{-1} for polymers 2, 3 and 4 and 23.5 kJ mol^{-1} for polymer 1. Generally, these results indicate an energetically homogeneous surface of the polymers.

Other nanoporous materials like MIF (aluminium-free ZSM-5 type zeolite), IRMOFs (isoreticular MOFs) and SWNT (single-wall carbon nanotubes) present heterogeneous surfaces so there exist significant differences in the heat of CO_2 adsorption at low and high loadings.[66] For MOFs with BET surface areas ranging from 1200 to 1600 $m^2\ g^{-1}$—that is, similar S_{BET} values to those reported here—higher heats of adsorption for CO_2 at low coverage were reported (~35 kJ mol^{-1}).[67] These were found to decrease to approximately 25 kJ mol^{-1} at higher gas loadings. Significant increases in the isosteric heat were observed for the adsorption of CO_2 in amine-grafted MOFs, particularly at very low loadings; a maximum value of Q_{st} of 90 kJ mol^{-1} was observed, indicating a strong and selective interaction of CO_2 with the amine functionalities.[68] This value compares well with previously reported data obtained for amine-functionalized silicas (100 kJ mol^{-1}).[69] High enthalpies at zero coverage were also observed for cation-exchanged zeolites such as NaX (49 kJ mol^{-1}) and Na-ZSM-5 (50 kJ mol^{-1}) that decrease with coverage to a plateau around 30 kJ mol^{-1}.[64]

Isosteric heats of CO_2 adsorption for these HCPs are similar to those obtained for activated carbons which have Q_{st} values of approximately 20.3 kJ mol^{-1},[70] reflecting the structural similarities between the two kinds of carbonaceous materials. Multi-wall carbon nanotubes (CNT) and amine-grafted CNT present average heats of CO_2 adsorption around 11.8 kJ mol^{-1} and 18.9 kJ mol^{-1},[71] respectively, lower than those assessed for HCPs and many kinds of zeolites.[72]

3.3. CO_2 capture capacity

CO_2 capture capacities of the prepared HCPs were evaluated at atmospheric and high pressures (up to 30 bar) at room temperature (298 K).

 This journal is © The Royal Society of Chemistry 2011

View Article Online

Published on 25 February 2011. Downloaded by Pennsylvania State University on 18/05/2016 03:58:11.

Table 3 Absolute density, ρ_{He}, and textural parameters calculated from the N_2 and CO_2 adsorption isotherms at 77 and 273 K, respectively[a]

		N_2 adsorption at 77 K				CO_2 adsorption at 273 K	
Sample	ρ_{He}	S_{BET}	V_p	V_{meso}	W_{0,N_2}	W_{0,CO_2}	L_{0,CO_2}
1	1.04	1646	1.26	0.51	0.66	0.27	0.9
2	0.93	1684	1.47	0.50	0.64	0.29	0.9
3	1.03	1531	1.44	0.40	0.60	0.28	0.9
4	1.09	1642	1.74	0.33	0.59	0.31	0.8
5	0.93	13	0.02	—	—	0.13	0.9
6	1.09	3	0.01	—	—	0.06	0.8
7	1.13	9	0.02	—	—	0.05	0.8

[a] ρ_{He} (g cm^{-3}): helium density; S_{BET} (m^2 g^{-1}): Brunauer, Emmet and Teller surface area; V_p (cm^3 g^{-1}): total pore volume; V_{meso} (cm^3 g^{-1}): mesopore volume (Hybrid DFT); W_{0,N_2} (cm^3 g^{-1}): total micropore volume at $p/p^0 < 0.1$ (DR equation); W_{0,CO_2} (cm^3 g^{-1}): narrow micropore volume at $p/p^0 < 0.01$ (DR equation) and L_{0,CO_2} (nm): average narrow micropore width (Stoeckli–Ballerini relation).

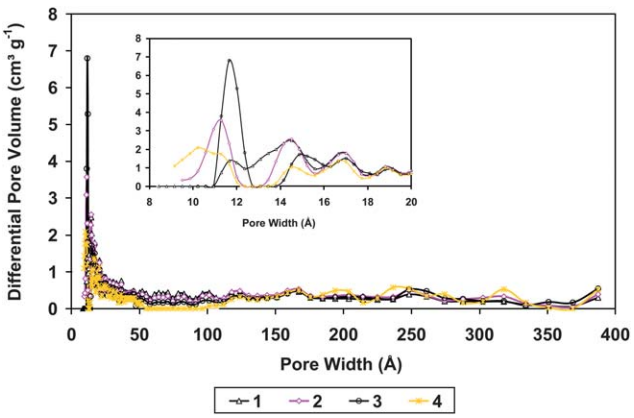

Fig. 4 Pore size distributions for HCPs (inset shows the detail of the micropore region).

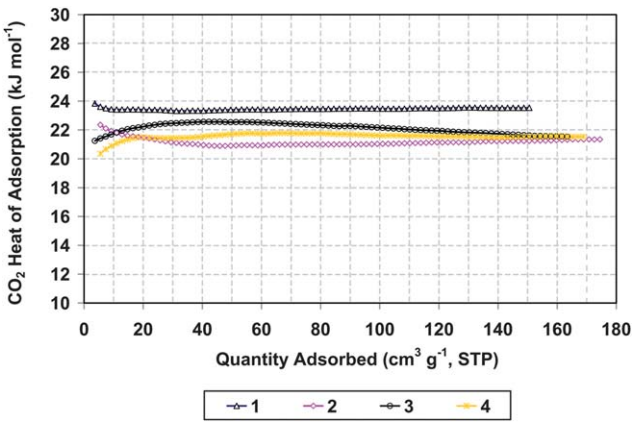

Fig. 5 Heats of adsorption of CO_2 for HCPs.

3.3.1. Atmospheric pressure tests. Fig. 6 shows the mass uptake of the samples during tests conducted on the TGA under a CO_2 flow (50 mL min^{-1}). CO_2 uptakes are expressed in terms of mass of CO_2 per mass of dry adsorbent. The HCPs show a CO_2 capture capacity of approximately 7 wt%. Due to their low textural development, the poorest performance corresponded to samples 5, 6 and 7 with CO_2 uptakes that do not exceed 2.5 wt% (0.6 mmol g^{-1}).

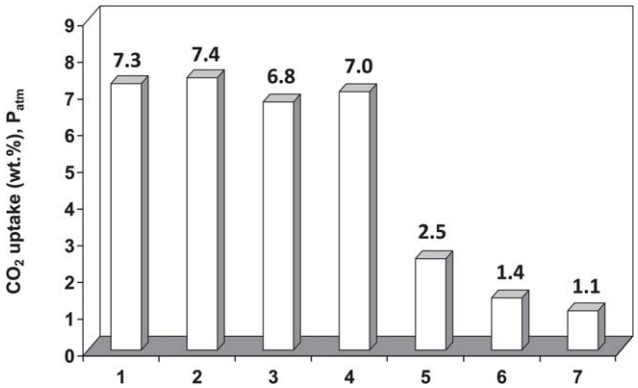

Fig. 6 CO_2 uptakes of the HCPs evaluated at atmospheric pressure and 298 K.

Fig. 7 shows that CO_2 uptakes at atmospheric pressure and ambient temperature seem to correlate better with narrow micropore volumes, W_{0,CO_2}, than with total micropore volumes, W_{0,N_2}. Microporous activated carbons from phenol–formaldehyde resins[73] have also been included in Fig. 7 to validate the correlation. HCPs fall below the fitted line in Fig. 7b, suggesting that experimental CO_2 capture capacities are lower than could be theoretically expected, according to their narrow micropore volume. CO_2 adsorption at atmospheric pressure is sensitive to the micropore width[20,21] and it has been demonstrated for activated carbons that micropore widths lower than 0.7 nm are the most active towards CO_2 capture at atmospheric pressure.[73] Thus, the presence of supermicropores (2 nm > micropore width > 0.7 nm) in these samples could account for the deviation from the fitted line (Fig. 7b).

3.3.2. High pressure tests. Fig. 8 presents the CO_2 and H_2 uptakes of some of the HCPs at 30 bar and 298 K. These values were obtained from the corresponding adsorption isotherms at 298 K. For polymers 1 to 4 the CO_2 adsorption capacity at 30 bar is significantly greater (by nearly two orders of magnitude) than the H_2 uptake. The highest value corresponded to polymer 1 with 0.1 wt% H_2 uptake; for the rest of the samples the values were insignificant in comparison with the CO_2 uptake. Therefore, the polymers may be selective to the separation of CO_2 from CO_2/H_2 mixtures (pre-combustion conditions). All tested polymers present significant CO_2 adsorption at 30 bar reaching values of

View Article Online

Published on 25 February 2011. Downloaded by Pennsylvania State University on 18/05/2016 03:58:11.

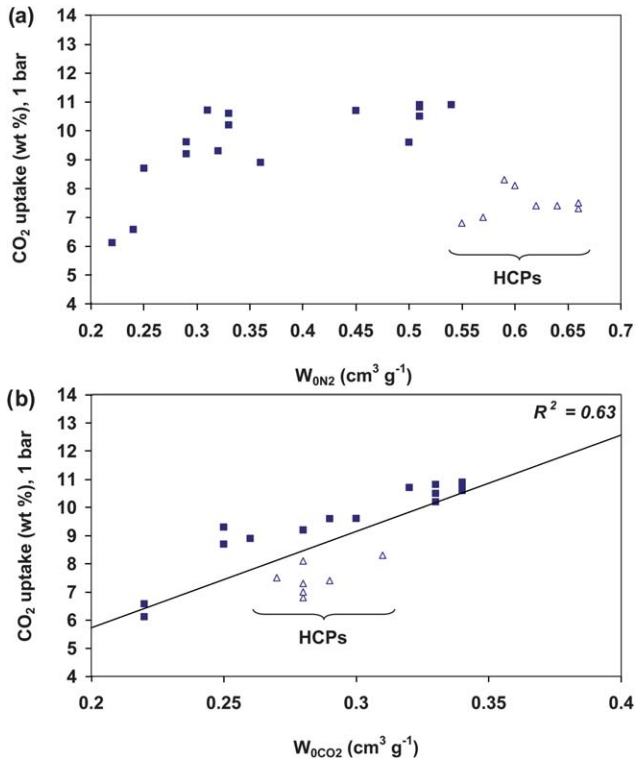

Fig. 7 Correlation of the CO_2 uptake at 1 bar with textural parameters (triangles: HCPs, squares: carbon-based adsorbents):[73] (a) total micropore volume, W_{0,N_2} and (b) narrow micropore volume, W_{0,CO_2}.

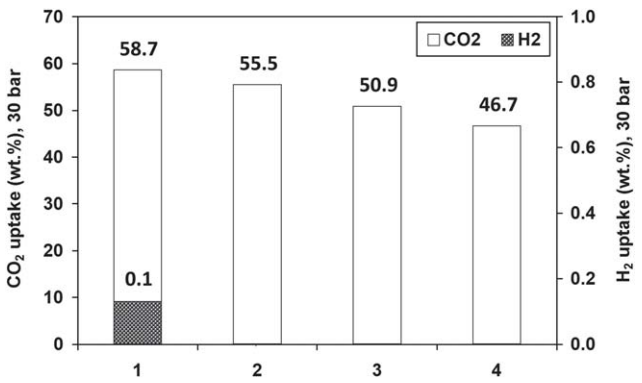

Fig. 8 CO_2 and H_2 uptakes of the HCPs evaluated at 30 bar and 298 K.

approximately 50 wt%. The maximum CO_2 uptake corresponded to sample 1 that reached 59 wt% (13.4 mmol g^{-1}). This polymer also exhibited the highest heat of CO_2 adsorption (see Fig. 5).

As for the atmospheric pressure tests, the CO_2 uptakes at 30 bar were related to the textural parameters of the polymers (Fig. 9). Contrary to the observed trend in the atmospheric pressure CO_2 capture tests, a good linear correlation exists between high pressure CO_2 uptakes and total micropore volume, W_{0,N_2}, of the polymers. Thus, CO_2 uptake at high pressure seems to depend on the total micropore volume, independently of the micropore size.

At atmospheric pressure the narrow micropore volume (pore sizes below 1.0 nm), evaluated by the CO_2 adsorption isotherm at 273 K, determines the maximum CO_2 uptake. This is not

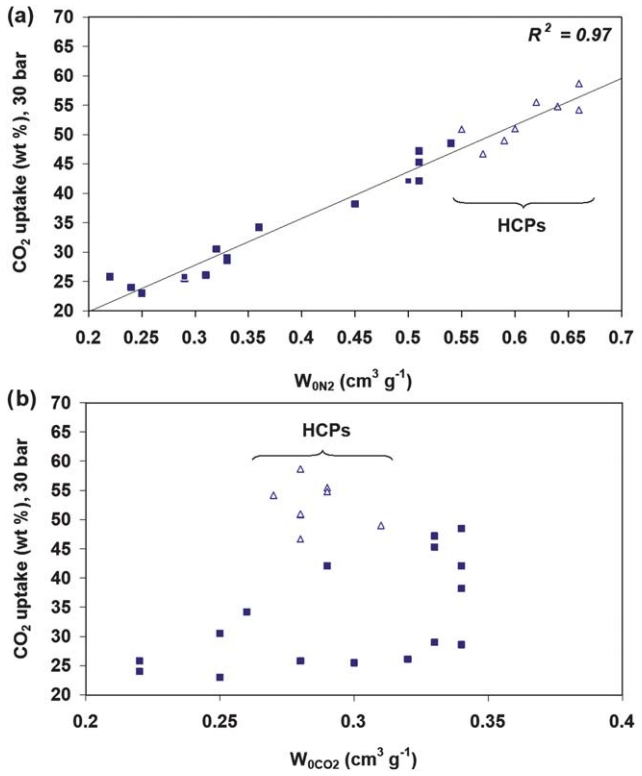

Fig. 9 Correlation of the CO_2 uptake at 30 bar with textural parameters (triangles: HCPs, squares: carbon-based adsorbents):[73] (a) total micropore volume, W_{0,N_2} and (b) narrow micropore volume, W_{0,CO_2}.

surprising since, as a consequence of the relatively high saturation pressure of CO_2, the process of CO_2 capture at low pressures corresponds to a small degree of pore filling which involves, exclusively, the narrower micropores in the carbons. At high pressure (30 bar) the total micropore volume, determined by the N_2 adsorption isotherm at 77 K, is the textural parameter more directly related to the CO_2 capacity of the materials. The good agreement revealed by Fig. 9a indicates that the retention of CO_2 under pre-combustion conditions (high pressures) occurs by filling of the entire microporosity. This is not accidental, because under such experimental conditions (298 K and 30 bar), CO_2 adsorption is close to saturation.

In Table 4, the CO_2 uptakes of the HCP polymers prepared in this work are compared with other CO_2 adsorbents that have shown promising performance. Most of the current literature on CO_2 physisorbents is based on zeolite-like materials and MOFs. The wide range of experimental conditions used to evaluate the CO_2 uptakes makes it difficult to make precise comparisons between different physisorbents. The selection of CO_2 adsorbents for particular applications is governed by the process design and desired process performance.

Selective adsorption of CO_2 on micro/mesoporous inorganic and organic adsorbents such as zeolites, silica gels, aluminas and activated carbons is used commercially for the separation of bulk CO_2 from a gas mixture and removal of trace CO_2 from a contaminated gas. Selective adsorption of CO_2 over gases like CO, CH_4, N_2, O_2 and H_2 by these materials is caused by van der Waals attraction between the CO_2 molecule and the adsorbent surface as well as by the pole–pole and pole–ion interactions

 This journal is © The Royal Society of Chemistry 2011

View Article Online

Published on 25 February 2011. Downloaded by Pennsylvania State University on 18/05/2016 03:58:11.

Table 4 CO_2 capture performance of adsorbent materials

Materials	CO_2 Heat of Adsorption/kJ mol^{-1}	CO_2 adsorption capacity/mmol g^{-1}	Conditions (*P*, *T*)	References
HCP 1	23.5	1.7	1 bar, 298 K	This work
		13.3	30 bar, 298 K	
HCP 2	21.2	1.7	1 bar, 298 K	This work
		12.6	30 bar, 298 K	
HCP 3	22.1	1.6	1 bar, 298 K	This work
		11.6	30 bar, 298 K	
HCP 4	21.6	1.6	1 bar, 298 K	This work
		10.6	30 bar, 298 K	
$Ni_2(BDC)_2Dabco^a$	20.4	12.5	15 bar, 298 K	74
		14.8	24 bar, 298 K	75
$Zn_2(BDC)_2Dabco^a$	21.6	2.1	1 bar, 298 K	74
		13.7	15 bar, 298 K	74
ZIF-70	—	2.2	1 bar, 298 K	67
USO-2-Ni	—	13.6	25 bar, 298K	75
USO-2-Ni-A^b	—	3.2	1 bar, 298 K	75
Zeolite 13X	37.2	7.4	32 bar, 298 K	19
		3.3	1 bar, 323 K	76
Zeolite NaX	49.0	7.8	30 bar, 302 K	77
AC-MAXSORB	16.2	25.0	35 bar, 298 K	78
		2.1	1 bar, 301 K	79
AC-Norit R1	22.0	10	30 bar, 298 K	77
AC-Norit RB2	—	9.5	40 bar, 298 K	32
BPL carbon	23.3	8.4	55 bar, 298 K	32
		1.9	1 bar, 298 K	67
		1.9	1 bar, 301 K	79
COF-102	—	27.3	55 bar, 298 K	32
MOF-177	35.0	32.5	30 bar, 298 K	35
		20.0	15 bar, 298 K	74
MOF-5(IRMOF-1)	34.1	1.9	1 bar, 298 K	76
		21.7	35 bar, 298 K	35
MCM-48^c	—	0.8	1 bar, 298 K	80
MIL-53(Al, Cr)^d	36.0	10	25 bar, 302 K	77
MIL-47(V)^d	—	11	20 bar, 302 K	77
PAF-1^e	—	29.5	40 bar, 298 K	83

^{a} Three dimensional pillared-layer-metal–organic framework. ^{b} Amine functionalized MOF. ^{c} A type of amine-attached silica. ^{d} MIL = materials of Institut Lavoisier (mesoporous MOFs). ^{e} Microporous polyphenylene network.

between the permanent quadrupole of the CO_2 molecules and the polar and ionic sites of the adsorbent surface. The varied morphology and surface chemistry of these physisorbents give rise to strikingly different characteristics for sorption of CO_2 as a pure gas or as a gas mixture. These materials show different adsorption capacities of CO_2 at a given gas pressure and temperature. In addition, the low to moderate isosteric heats of adsorption of these adsorbents permit reversible adsorption of CO_2 and relatively easier desorption of CO_2 from these materials. In particular, zeolites exhibit extremely high capacity for CO_2 at a very low pressure because of the very strong quadrupole-ion interaction. Physical adsorption of CO_2 by microporous zeolite 13X has been reported to provide high CO_2 adsorption capacity at ambient temperature, but there is a relatively high energy requirement for regeneration, especially in the presence of water.[19]

Recently, a range of microporous crystalline zeolite analogues has been developed, in particular, metal–organic frameworks (MOFs), covalent organic frameworks (COFs) and zeolitic imidazolate frameworks (ZIFs) that exhibit exceptional uptakes and selectivity to CO_2. MOFs and COFs present very large specific surface areas (>3000 m^2 g^{-1}, ref. 32) but in some cases limited physicochemical stability. On the other hand, ZIFs present lower surface areas (up to 1700 m^2 g^{-1}, ref. 67) but higher chemical stabilities. Several groups have reported MOFs that have high CO_2 adsorption capacity at ambient temperature under dry conditions.[35,75,77]

Amorphous microporous organic polymers have received recent interest in gas storage applications.[40,56,81,82] They present surface areas up to 1900 m^2 g^{-1} (ref. 40) with the exception of the recently reported PAF-1 that exhibits a BET surface area >5000 m^2 g^{-1}.[83] Capture capacities at atmospheric pressure and room temperature of the tested HCPs are similar to other carbon-based adsorbents, like commercial activated carbons,[79,67] higher than some MOFs[74,76] and lower than zeolite 13X[76] and amine-functionalized MOFs.[75] At higher pressures (~30 bar) these HCPs reached capture capacities superior to zeolite-based adsorbents[19,77] and activated carbons[77] but inferior to PAF-1,[83] and the highest surface area MOFs and COFs. However, taking into account the low isosteric heat of CO_2 adsorption and the selectivity towards CO_2 of these HCPs, they may be suitable candidates for pre-combustion capture applications where high CO_2 partial pressures are involved.

4. Conclusions

A series of hypercrosslinked polymers has been characterized and tested for CO_2 capture. HCPs synthesized using DCE as solvent presented suitable microporosity development for CO_2 adsorption purposes. However, use of cyclohexane, *n*-hexane

View Article Online

Published on 25 February 2011. Downloaded by Pennsylvania State University on 18/05/2016 03:58:11.

and dodecane as solvents resulted in negligible textural development. CO_2 capture capacities where evaluated in pure CO_2 under atmospheric and high pressures and room temperature. Maximum CO_2 uptakes of up to 13.4 mmol g^{-1} (59 wt%) at 298 K and 30 bar were reached.

CO_2 capture capacities of the HCPs are comparable to those of high-surface area adsorbents found in the literature. In addition, these polymers are relatively inexpensive and present low isosteric heats of CO_2 adsorption and good selectivity towards CO_2. Thus, HCPs synthesized in this work show promising characteristics to be applied in pre-combustion CO_2 capture processes by means of PSA cycles.

Acknowledgements

We are grateful for funding to EPSRC *via* EP/G061785/1 and to MICINN *via* Project ENE2008-05087. C.F.M. is grateful to the CSIC JAE-Predoc Program, co-financed by the European Social Fund, for funding a short stay at the Department of Chemistry, University of Liverpool. A.I.C. is a Royal Society Wolfson Merit Award holder.

References

1 J. D. Figueroa, T. Fout, S. Plasynski, H. McIlvried and R. D. Srivastava, *Int. J. Greenhouse Gas Control*, 2008, **2**, 9–20.
2 A. D. Ebner and J. A. Ritter, *Sep. Sci. Technol.*, 2009, **44**, 1273–1421.
3 G. P. Knowles, J. V. Graham, S. W. Delaney and A. L. Chaffee, *Fuel Process. Technol.*, 2005, **86**, 1435–1448.
4 M. L. Gray, Y. Soong, K. J. Champagne, J. Baltrus, R. W. Stevens, Jr, P. Toochinda and S. S. C. Chuang, *Sep. Purif. Technol.*, 2004, **35**, 31–36.
5 X. Xu, C. Song, J. M. Andresen, B. G. Miller and A. W. Scaroni, *Microporous Mesoporous Mater.*, 2003, **62**, 29–45.
6 T. Filburn, J. J. Helble and R. A. Weiss, *Ind. Eng. Chem. Res.*, 2005, **44**, 1542–1546.
7 M. Radosz, X. Hu, K. Krutkramelis and Y. Shen, *Ind. Eng. Chem. Res.*, 2008, **47**, 3783–3794.
8 M. M. Maroto-Valer, Z. Tang and Y. Zhang, *Fuel Process. Technol.*, 2005, **86**, 1487–1502.
9 M. G. Plaza, C. Pevida, A. Arenillas, F. Rubiera and J. J. Pis, *Fuel*, 2007, **86**, 2204–2212.
10 C. Lu, H. Bai, B. Wu, F. Su and J. F. Hwang, *Energy Fuels*, 2008, **22**, 3050–3056.
11 C. Pevida, M. G. Plaza, B. Arias, J. Fermoso, F. Rubiera and J. J. Pis, *Appl. Surf. Sci.*, 2008, **254**, 7165–7172.
12 M. G. Plaza, C. Pevida, B. Arias, M. D. Casal, C. F. Martín, J. Fermoso, F. Rubiera and J. J. Pis, *J. Environ. Eng.*, 2009, **135**, 426–432.
13 C. Pevida, T. C. Drage and C. E. Snape, *Carbon*, 2008, **46**, 1464–1474.
14 T. C. Drage, J. M. Blackman, C. Pevida and C. E. Snape, *Energy Fuels*, 2009, **23**, 2790–2796.
15 T. Nelson, L. Coleman, M. Anderson, J. Herr and M. Pavani, in *Annual NETL CO_2 Capture Technology for Existing R&D Meeting*, Pittsburgh, 2009.
16 N. Shigemoto, T. Yanagihara, S. Sugiyama and H. Hayashi, *Energy Fuels*, 2006, **20**, 721–726.
17 J. Merel, M. Clausse and F. Meunier, *Ind. Eng. Chem. Res.*, 2008, **47**, 209–215.
18 D. Ko, R. Siriwardane and L. T. Biegler, *Ind. Eng. Chem. Res.*, 2003, **42**, 339–348.
19 S. Cavenati, C. A. Grande and A. E. Rodrigues, *J. Chem. Eng. Data*, 2004, **49**, 1095–1101.
20 J. M. Martin-Martinez, R. Torregrosa-Macia and M. C. Mittelmeijer-Hazeleger, *Fuel*, 1995, **74**, 111–114.
21 A. Vishnyakov, P. I. Ravikovitch and A. V. Neimark, *Langmuir*, 1999, **15**, 8736–8742.
22 D. Cazorla-Amoros, J. Alcaniz-Monge and A. Linares-Solano, *Langmuir*, 1996, **12**, 2820–2824.
23 J. A. Ritter and A. D. Ebner, *Sep. Sci. Technol.*, 2007, **42**, 1123–1193.
24 J. Yang, C.-H. Lee and J.-W. Chang, *Ind. Eng. Chem. Res.*, 1997, **36**, 2789–2798.
25 C. Song, *Catal. Today*, 2006, **115**, 2–32.
26 X. Xiaoding and J. A. Moulijn, *Energy Fuels*, 1996, **10**, 305–325.
27 J. F. Jenck, F. Agterberg and M. J. Droescher, *Green Chem.*, 2004, **6**, 544–556.
28 J. M. Austell, *Exploration and Production: the Oil and Gas Review*, 2005.
29 J. Schell, N. Casas and M. Mazzotti, *Energy Proc.*, 2009, **1**, 655–660.
30 P. Xiao, S. Wilson, G. Xiao, R. Singh and P. Webley, *Energy Proc.*, 2009, **1**, 631–638.
31 D. Britt, H. Furukawa, B. Wang, T. G. Glover and O. M. Yaghi, *Proc. Natl. Acad. Sci. U. S. A.*, 2009, **106**, 20637–20640.
32 H. Furukawa and O. M. Yaghi, *J. Am. Chem. Soc.*, 2009, **131**, 8875–8883.
33 S. Choi, J. H. Drese and C. W. Jones, *ChemSusChem*, 2009, **2**, 796–854.
34 H. Hayashi, A. P. Cote, H. Furukawa, M. O'Keeffe and O. M. Yaghi, *Nat. Mater.*, 2007, **6**, 501–506.
35 A. R. Millward and O. M. Yaghi, *J. Am. Chem. Soc.*, 2005, **127**, 17998–17999.
36 J.-X. Jiang and A. I. Cooper, *Top. Curr. Chem.*, 2009, **293**, 1–33.
37 M. P. Tsyurupa and V. A. Davankov, *React. Funct. Polym.*, 2002, **53**, 193–203.
38 M. P. Tsyurupa and V. A. Davankov, *React. Funct. Polym.*, 2006, **66**, 768–779.
39 V. A. Davankov and M. P. Tsyurupa, *React. Polym.*, 1990, **13**, 27–42.
40 C. D. Wood, B. Tan, A. Trewin, H. Niu, D. Bradshaw, M. J. Rosseinsky, Y. Z. Khimyak, N. L. Campbell, R. Kirk, E. Stockel and A. I. Cooper, *Chem. Mater.*, 2007, **19**, 2034–2048.
41 J. Y. Lee, C. D. Wood, D. Bradshaw, M. J. Rosseinsky and A. I. Cooper, *Chem. Commun.*, 2006, 2670–2672.
42 N. B. McKeown, P. M. Budd, K. J. Msayib, B. S. Ghanem, H. J. Kingston, C. E. Tattershall, S. Makhseed, K. J. Reynolds and D. Fritsch, *Chem.–Eur. J.*, 2005, **11**, 2610–2620.
43 N. B. McKeown and P. M. Budd, *Chem. Soc. Rev.*, 2006, **35**, 675–683.
44 J.-X. Jiang, F. Su, A. Trewin, C. D. Wood, N. L. Campbell, H. Niu, C. Dickinson, A. Y. Ganin, M. J. Rosseinsky, Y. Z. Khimyak and A. I. Cooper, *Angew. Chem., Int. Ed.*, 2007, **46**, 8574–8578.
45 E. Stöckel, X. F. Wu, A. Trewin, C. D. Wood, R. Clowes, N. L. Campbell, J. T. A. Jones, Y. Z. Khimyak, D. J. Adams and A. I. Cooper, *Chem. Commun.*, 2009, 212–214.
46 R. Dawson, A. Laybourn, R. Clowes, Y. Z. Khimyak, D. J. Adams and A. I. Cooper, *Macromolecules*, 2009, **42**, 8809–8816.
47 A. I. Cooper, *Adv. Mater.*, 2009, **21**, 1291–1295.
48 V. A. Davankov, S. V. Rogozhin and M. P. Tsyurupa, *US Pat.*, 3729457, 1971.
49 S. N. Sidorov, L. M. Bronstein, V. A. Davankov, M. P. Tsyurupa, S. P. Solodovnikov, P. M. Valetsky, E. A. Wilder and R. J. Spontak, *Chem. Mater.*, 1999, **11**, 3210–3215.
50 V. A. Davankov, A. V. Pastukhov and M. P. Tsyurupa, *J. Polym. Sci., Part B: Polym. Phys.*, 2000, **38**, 1553–1563.
51 A. V. Pastukhov, M. P. Tsyurupa and V. A. Davankov, *J. Polym. Sci., Part B: Polym. Phys.*, 1999, **37**, 2324–2333.
52 J.-H. Ahn, J.-E. Jang, C.-G. Oh, S.-K. Ihm, J. Cortez and D. C. Sherrington, *Macromolecules*, 2006, **39**, 627–632.
53 V. V. Podlesnyuk, J. Hradil and E. Králová, *React. Funct. Polym.*, 1999, **42**, 181–191.
54 A. Li, Q. Zhang, G. Zhang, J. Chen, Z. Fei and F. Liu, *Chemosphere*, 2002, **47**, 981–989.
55 N. A. Penner, P. N. Nesterenko, M. M. Ilyin, M. P. Tsyurupa and V. A. Davankov, *Chromatographia*, 1999, **50**, 611–620.
56 A. Trewin, D. J. Willock and A. I. Cooper, *J. Phys. Chem. C*, 2008, **112**, 20549–20559.
57 R. Dawson, A. Laybourn, Y. Z. Khimyak, D. J. Adams and A. I. Cooper, *Macromolecules*, 2010, **43**, 8524–8530.
58 D. C. Sherrington, *Chem. Commun.*, 1998, 2275–2286.
59 M. M. Dubinin, *Carbon*, 1989, **27**, 457–467.
60 J. P. Olivier, S. Koch, M. Jaroniec and M. Kruk, *Characterization of Porous Solids V*, Elsevier, Amsterdam, 2000.
61 F. Stoeckli and L. Ballerini, *Fuel*, 1991, **70**, 557–559.
62 S. Brunauer, L. S. Deming, W. E. Deming and E. Teller, *J. Am. Chem. Soc.*, 1940, **62**, 1723–1732.
63 S. Sircar, *Appl. Surf. Sci.*, 2005, **252**, 647–653.

 This journal is © The Royal Society of Chemistry 2011

View Article Online

Published on 25 February 2011. Downloaded by Pennsylvania State University on 18/05/2016 03:58:11.

64 J. A. Dunne, R. Mariwala, M. Rao, S. Sircar, R. J. Gorte and A. L. Myers, *Langmuir*, 1996, **12**, 5888–5895.
65 S. Sircar and D. V. Cao, *Chem. Eng. Technol.*, 2002, **25**, 945–948.
66 R. Babarao and J. Jiang, *Langmuir*, 2008, **24**, 6270–6278.
67 A. Phan, C. J. Doonan, F. J. Uribe-Romo, C. B. Knobler, M. O'keeffe and O. M. Yaghi, *Acc. Chem. Res.*, 2010, **43**, 58–67.
68 A. Demessence, D. M. D'Alessandro, M. L. Foo and J. R. Long, *J. Am. Chem. Soc.*, 2009, **131**, 8784–8786.
69 C. Knöfel, J. Descarpentries, A. Benzaouia, V. Zelenák, S. Mornet, P. L. Llewellyn and V. Hornebecq, *Microporous Mesoporous Mater.*, 2007, **99**, 79–85.
70 I. A. A. C. Esteves, M. S. S. Lopes, P. M. C. Nunes and J. P. B. Mota, *Sep. Purif. Technol.*, 2008, **62**, 281–296.
71 S.-C. Hsu, C. Lu, F. Su, W. Zeng and W. Chen, *Chem. Eng. Sci.*, 2010, **65**, 1354–1361.
72 R. V. Siriwardane, M.-S. Shen and E. P. Fisher, *Energy Fuels*, 2005, **19**, 1153–1159.
73 C. F. Martín, M. G. Plaza, J. J. Pis, F. Rubiera, C. Pevida and T. A. Centeno, *Sep. Purif. Technol.*, 2010, **74**, 225–229.
74 Z. Liang, M. Marshall and A. L. Chaffee, *Microporous Mesoporous Mater.*, 2010, **132**, 305–310.
75 B. Arstad, H. Fjellvåg, K. Kongshaug, O. Swang and R. Blom, *Adsorption*, 2008, **14**, 755–762.
76 Z. Zhao, Z. Li and Y. S. Lin, *Ind. Eng. Chem. Res.*, 2009, **48**, 10015–10020.
77 P. L. Llewellyn, S. Bourrelly, C. Serre, A. Vimont, M. Daturi, L. Hamon, G. de Weireld, J.-S. Chang, D.-Y. Hong, Y. Kyu Hwang, S. Hwa Jhung and G. Férey, *Langmuir*, 2008, **24**, 7245–7250.
78 S. Himeno, T. Komatsu and S. Fujita, *J. Chem. Eng. Data*, 2005, **50**, 369–376.
79 K. B. Lee, M. G. Beaver, H. S. Caram and S. Sircar, *Ind. Eng. Chem. Res.*, 2008, **47**, 8048–8062.
80 S. Kim, J. Ida, V. V. Guliants and J. Y. S. Lin, *J. Phys. Chem. B*, 2005, **109**, 6287–6293.
81 C. D. Wood, B. Tan, A. Trewin, F. Su, M. J. Rosseinsky, D. Bradshaw, Y. Sun, L. Zhou and A. I. Cooper, *Adv. Mater.*, 2008, **20**, 1916–1921.
82 N. B. McKeown, B. Gahnem, K. J. Msayib, P. M. Budd, C. E. Tattershall, K. Mahmood, S. Tan, D. Book, H. W. Langmi and A. Walton, *Angew. Chem., Int. Ed.*, 2006, **45**, 1804–1807.
83 T. Ben, H. Ren, S. Ma, D. Cao, J. Lan, X. Jing, W. Wang, J. Xu, F. Deng, J. Simmons, S. Qiu and G. Zhu, *Angew. Chem.*, 2009, **121**, 9621–9624.